

## Electronic Supplementary Information

### Controlled evaporative self-assembly of Fe<sub>3</sub>O<sub>4</sub> nanoparticles assisted by external magnetic field

Yonghong Men,<sup>a,b</sup> Wenqin Wang,<sup>\*a</sup> Peng Xiao,<sup>b</sup> Jincui Gu,<sup>b</sup> Aihua Sun,<sup>b</sup> Youju Huang,<sup>b</sup> Jiawei Zhang<sup>\*b</sup> and Tao Chen<sup>\*b</sup>

<sup>a</sup>Faculty of Materials Science and Chemical Engineering, Ningbo University, Ningbo 315211, China

<sup>b</sup>Division of Polymer and Composite Materials, Ningbo Institute of Material Technology and Engineering, Chinese Academy of Science, 1219 Zhongguan West Road, Ningbo 315201, China

Received (in XXX, XXX) Xth XXXXXXXXXX 20XX, Accepted Xth XXXXXXXXXX 20XX  
DOI: 10.1039/b000000x

**Self-initiated photografting and photopolymerization (SIPGP):** The phenomenon of SIPGP on various kinds of substrates has been reported very early.<sup>1, 2</sup> During SIPGP process, the monomer itself can be acted as photosensitizer to create a free-radical site resulting in the surface-initiated free-radical grafting reaction on photoactive surface. The patterned polymer brushes can be fabricated without a surface bound initiator by SIPGP due to its several advantages. For example, no additional surface analog reaction is required to graft a photoinitiator, and layered brushes from different vinyl monomers can be formed by consecutive SIPGP, and polymer brushes are introduced to surface via C–C or C–X-bonds.<sup>3</sup>

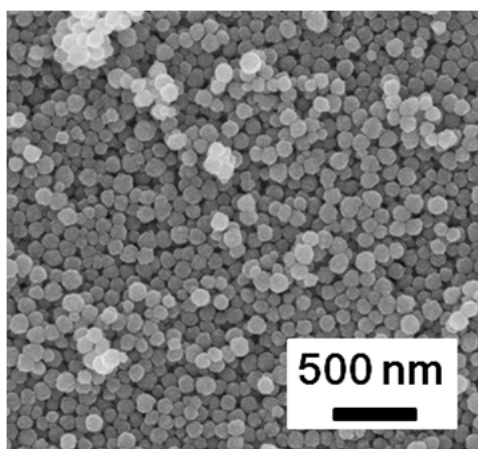


**Fig. S1** SEM image of Fe<sub>3</sub>O<sub>4</sub> NPs.

In order to confirm TMSPMA grafting on the surface of  $\text{Fe}_3\text{O}_4$  NPs, FTIR was performed. As shown in **Fig. S2**, in the spectrum of TMSPMA-modified  $\text{Fe}_3\text{O}_4$  NPs, the band at  $580\text{ cm}^{-1}$  is the characteristic absorption band of  $\text{Fe}_3\text{O}_4$ .<sup>4</sup> The stretching vibration of  $-\text{CH}_2-$  and  $-\text{CO}-$  are about at  $2920\text{ cm}^{-1}$  and  $1714\text{ cm}^{-1}$ , respectively. The bands at  $1628\text{ cm}^{-1}$  and  $1111\text{ cm}^{-1}$  are assigned to the Si-O and C=C, respectively.<sup>4</sup> The FTIR results confirm that TMSPMA was successfully introduced onto the surface of  $\text{Fe}_3\text{O}_4$  NPs.

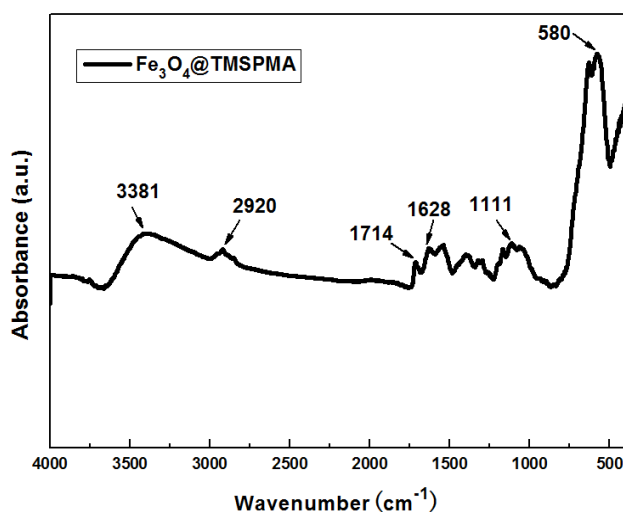


**Fig. S2** FTIR spectrum of  $\text{Fe}_3\text{O}_4@TMSPMA$ .

During the process of CESA assisted by magnetic field, temperature not only affects the formation of stripes along magnetic field direction, but also affects the formation of concentric rings (perpendicular to magnetic field direction). As shown in **Fig. S3**, with increasing temperature, the formation of concentric rings is becoming better. However, when temperature was too higher, it is not favorable to the formation of concentric rings due to higher evaporative rate.

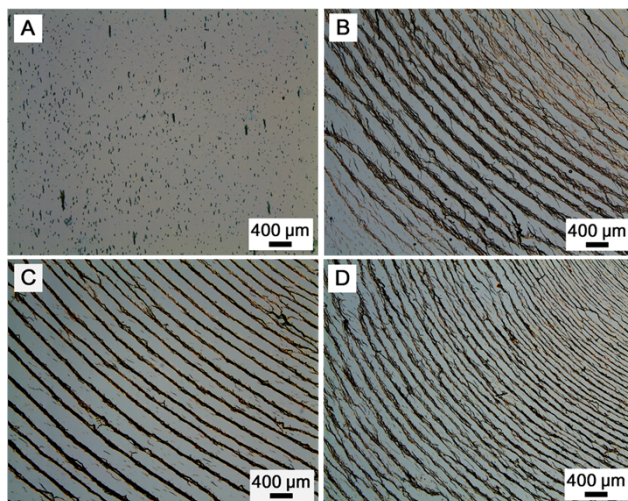


**Fig. S3** Optical micrograph images of  $\text{Fe}_3\text{O}_4$  NPs patterns under different temperatures (room temperature for A, 40 °C for B, 50 °C for C, 60 °C for D) with static magnetic field  $f = 0$  rpm (perpendicular to magnetic field direction).

In order to further characterize the surface morphologies of  $\text{Fe}_3\text{O}_4$  NPs patterns with different magnetic field rotation frequency, SEM was performed. As shown in **Fig. S4**, the results are consistent with morphologies characterized by optical microscope. The self-assembly along magnetic field gradually disappears with increasing magnetic field rotation frequency. In addition, there are some  $\text{Fe}_3\text{O}_4$  NPs between adjacent concentric rings resulting in some small self-assembly morphologies between adjacent concentric rings (**Fig. S4C, S4D**).

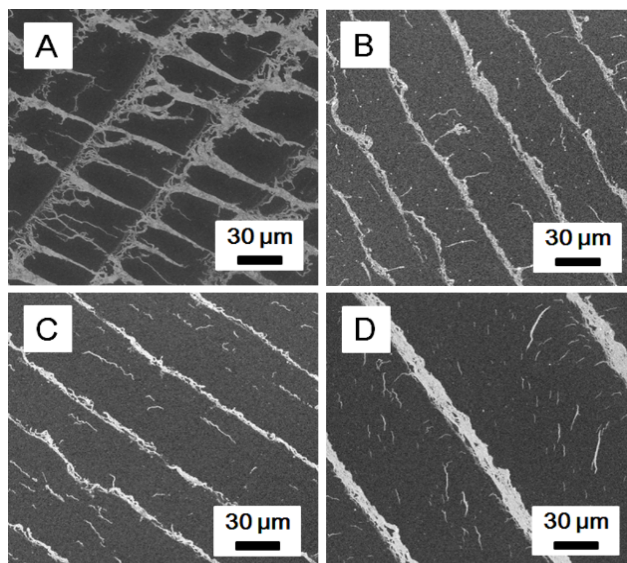


**Fig. S4** SEM images of  $\text{Fe}_3\text{O}_4$  NPs patterns with different magnetic field rotation frequency (0 rpm for A, 100 rpm for B, 200 rpm for C, 300 rpm for D) at 50 °C.

During the process of self-assembly of  $\text{Fe}_3\text{O}_4$  NPs via magnetic field assisted CESA, the concentration of  $\text{Fe}_3\text{O}_4$  NPs also plays an important role in the evaporation process. As shown in **Fig. S5**, increasing the concentration is favorable for the formation of linear stripes along magnetic field direction (**Fig. S5A, S5C and S5E**), which is because of the dipole-dipole interactions between adjacent  $\text{Fe}_3\text{O}_4$  NPs increased with increasing concentration. On the other hand, increasing the concentration leads to more  $\text{Fe}_3\text{O}_4$  NPs deposition in contact line, which will promote the formation of concentric rings (**Fig. S5B, S5D and S5F**). The average width of ring is changed from 4  $\mu\text{m}$  to 6  $\mu\text{m}$  and 7  $\mu\text{m}$ , and the average spacing of ring is changed from 45  $\mu\text{m}$  to 37  $\mu\text{m}$  and 27  $\mu\text{m}$ , at the same time, the average width of the stripes is increased from 3  $\mu\text{m}$  to 4  $\mu\text{m}$  and 7  $\mu\text{m}$ , corresponding to 0.05 mg/mL, 0.1 mg/mL, and 0.2 mg/mL of  $\text{Fe}_3\text{O}_4$  NPs solution, respectively.

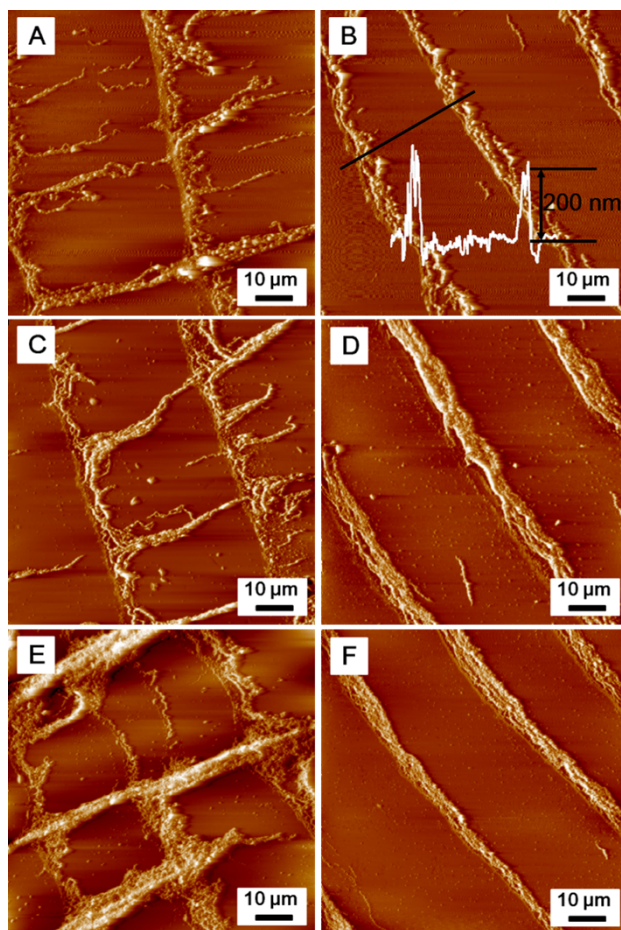


**Fig. S5** AFM height images of  $\text{Fe}_3\text{O}_4$  NPs patterns with different concentrations (0.05 mg/mL for A and B, 0.1 mg/mL for C and D, 0.2 mg/mL for E and F) under the optimal temperature ( $T = 50^\circ\text{C}$ ) and static magnetic field ( $f = 0$  rpm) (A, C and E, along magnetic field direction, B, D and F, perpendicular to magnetic field direction).

SEM was employed to further characterize the surface morphologies of  $\text{Fe}_3\text{O}_4$  NPs patterns with different concentrations. As shown in **Fig. S6**, all of stripes and concentric rings are become better with increasing concentrations. At the same time, the accumulation of  $\text{Fe}_3\text{O}_4$  NPs becomes more compact.

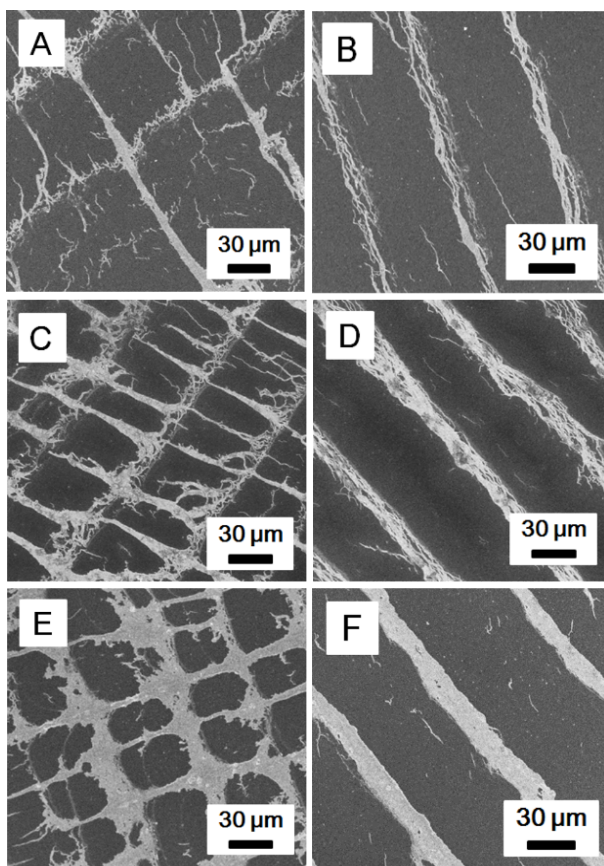


**Fig. S6** SEM images of  $\text{Fe}_3\text{O}_4$  NPs patterns with different concentrations (0.05 mg/mL for A and B, 0.1 mg/mL for C and D, 0.2 mg/mL for E and F) under the optimal temperature ( $T = 50\text{ }^\circ\text{C}$ ) and static magnetic field ( $f = 0\text{ rpm}$ ) (A, C and E, along magnetic field direction, B, D and F, perpendicular to magnetic field direction).

In order to scrutinize the surface morphology of  $\text{Fe}_3\text{O}_4$  NPs after SIPGP, AFM and SEM were employed (**Fig. S7**). The height of PS brushes is about 230 nm (**Fig. S7A**). The polymer brushes grafted  $\text{Fe}_3\text{O}_4$  NPs can be further lifted off from the silicon substrate using alkaline media as etching agent (**Fig. S7B**). PS brushes were grafted on the surface of  $\text{Fe}_3\text{O}_4$  NPs, therefore the spherical morphology is not clearly seen (**Fig. S7C** and **S7D**).

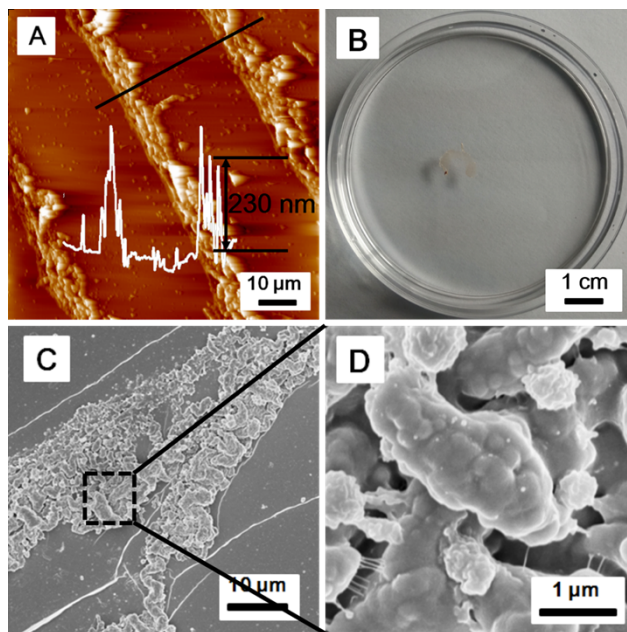


**Fig. S7** (A) AFM image of PS brushes. (B) The free-standing film floating on the surface of water. (C) SEM images of the front side of free-standing film. (D) The close-up SEM image of (C).

As shown in **Movie S1**, the free-standing film could float on the water surface. In addition, although  $\text{Fe}_3\text{O}_4$  NPs were encapsulated by PS, the magnetic property was not changed. Therefore, the free-standing film can move on the water surface with the movement of a magnet.

1 H. S. Taylor and A. A. Vernon, *J. Am. Chem. Soc.*, 1931, **53**, 2527-2536.

2 A. N. Wright, *Nature*, 1967, **215**, 953-955.

3 T. Chen, I. Amin and R. Jordan, *Chem. Soc. Rev.*, 2012, **41**, 3280-3296.

4 T. Y. Chen, Z. Cao, X. L. Guo, J. J. Nie, J. T. Xu, Z. Q. Fan and B. Y. Du, *Polymer*, 2011, **52**, 172-179.